Ahad James (Orcid ID: 0000-0003-2415-2343)
Liu Yuchi (Orcid ID: 0000-0003-3533-1697)
Fyrdahl Alexander (Orcid ID: 0000-0003-0237-7699)
Hamilton Jesse Ian (Orcid ID: 0000-0002-4463-481X)
Franson Dominique (Orcid ID: 0000-0002-9870-3147)

Author Manuscript

TITLE PAGE

Self-calibrated through-time spiral GRAPPA for real-time, free-breathing evaluation of left ventricular function

Dominique Franson[1], James Ahad[1], Yuchi Liu[2], Alexander Fyrdahl[2], William Truesdell[2], Jesse Hamilton[2], Nicole Seiberlich[2]

[1]Case Western Reserve University

Department of Biomedical Engineering

Wickenden Building

10900 Euclid Avenue

Cleveland, OH, USA 44106-7078

[2]University of Michigan

Department of Radiology

Medical Science Research Building II

1500 E Medical Center Drive

Ann Arbor, MI 48109

Corresponding author:

Dr. Nicole Seiberlich

Email: nse@med.umich.edu

Running head: Self-calibrated through-time spiral GRAPPA for real-time, free-breathing evaluation of left ventricular function

Word count:

Main body: 5409/5000

Abstract: 249/250

Figures and tables: 10/10

Supplementary figures: 7

This is the author manuscript accepted for publication and has undergone full peer review but has not been through the copyediting, typesetting, pagination and proofreading process, which may lead to differences between this version and the Version of Record. Please cite this article as doi: 10.1002/mrm.29462

This article is protected by copyright. All rights reserved.

Supplementary videos: 9

Author Manuscript

Author Manuscript

ABSTRACT

Purpose

Through-time spiral GRAPPA is a real-time imaging technique that enables ungated, free-breathing evaluation of the left ventricle. However, it requires a separate fully-sampled calibration scan to calculate GRAPPA weights. A self-calibrated through-time spiral GRAPPA method is proposed that uses a specially designed spiral trajectory with interleaved arm ordering such that consecutive undersampled frames can be merged to form calibration data, eliminating the separate fully-sampled acquisition.

Methods

The proposed method considers the time needed to acquire data at all points in a GRAPPA calibration kernel when using interleaved arm ordering. Using this metric, simulations were performed to design a spiral trajectory for self-calibrated GRAPPA. Data were acquired in healthy volunteers using the proposed method and a comparison electrocardiogram-gated and breath-held cine scan. Left ventricular functional values and image quality are compared.

Results

A 12-arm spiral trajectory was designed with a temporal resolution of 32.72 ms/cardiac phase with an acceleration factor of 3. Functional values calculated using the proposed method and the gold-standard method were not statistically significantly different (paired t-test, $p<0.05$). Image quality ratings were lower for the proposed method, with statistically significantly different ratings (Wilcoxon signed rank test, $p<0.05$) for two of five image quality aspects rated (level of artifact, blood-myocardium contrast).

Conclusions

A self-calibrated through-time spiral GRAPPA reconstruction can enable ungated, free-breathing evaluation of the left ventricle in 71 seconds. Functional values are equivalent to a gold-standard cine technique, although some aspects of image quality may be inferior due to the real-time nature of the data collection.

Keywords: parallel imaging, non-Cartesian, GRAPPA, real-time, spiral, cardiovascular magnetic resonance

Author Manuscript

INTRODUCTION

Cardiac magnetic resonance imaging (MRI) can be used to evaluate left ventricular structure and function. These features are commonly assessed using cine datasets[1,2] with high spatial and temporal resolution. Although the final cine images depict cardiac motion over a single heartbeat, these data are typically acquired over multiple heartbeats with electrocardiogram (ECG) gating to guide adequate data acquisition at each cardiac phase. Because data collection occurs over multiple heartbeats, conventional cine acquisitions require a regular heart rate with ECG gating and multiple breath-holds. These requirements may be challenging for patients with arrhythmias or who have difficulty with breath-holds.

Another option for functional cardiac imaging is to use real-time imaging, in which data are acquired quickly enough that an entire image can be captured without sharing data across different heartbeats. Many approaches have been proposed to enable real-time cardiac imaging[3–5]. Most use data undersampling to reach the desired spatiotemporal resolutions, combined with an image reconstruction method to remove aliasing artifacts. Reconstruction methods include parallel imaging[6–8], k-t methods[9], nonlinear inverse reconstructions[10,11], sparse reconstructions including compressed sensing[12], and, deep learning reconstructions[13].

Through-time radial GRAPPA is one non-Cartesian parallel imaging method that has been proposed for real-time acquisition and reconstruction[14,15]. Undersampled radial data are acquired in a free-running fashion, without ECG synchronization. Through-time radial GRAPPA[14] is then used to reconstruct unaliased images. Aandal et al[16] evaluated this method for left ventricular (LV) evaluation in 63 patients. Ejection fraction (EF), end diastolic volume (EDV), and end systolic volume (ESV) values were not statistically significantly different from values calculated using the gold-standard method. Through-time non-Cartesian GRAPPA has also been developed for spiral trajectories, which can be used to acquire data more efficiently than radial trajectories, enabling higher frame rates with lower acceleration factors[17].

Although through-time GRAPPA is a promising technique for real-time LV evaluation[16,18], one drawback is that separate, fully-sampled calibration data must be acquired. For multi-slice scans like those used for LV evaluation, a calibration dataset is needed for each slice. For example, the

Author Manuscript

original implementation of through-time spiral GRAPPA used ~18s of calibration data per slice[17], or 216s of calibration scanning for 12 slices. To reduce total scan time, it would be beneficial to remove this separate calibration dataset, and perform GRAPPA with calibration data derived from the undersampled data in a self-calibrated fashion.

In this work we propose a self-calibrated through-time spiral GRAPPA method that uses an interleaved undersampling pattern to remove the separate calibration dataset. Consecutive undersampled frames are merged to form fully-sampled calibration frames. The standard through-time spiral GRAPPA calibration and reconstruction processes are then performed. This approach is similar to TGRAPPA[6], in which an interleaved Cartesian acquisition is used to build up calibration frames over time, but adapted for a non-Cartesian trajectory. Hamilton et al previously presented a TGRAPPA-inspired method for spiral trajectories[19]. The same trajectory used for conventional, separately-calibrated through-time spiral GRAPPA was used for the self-calibrating version. Accurate reconstructions were generated for slow and moderate cardiac motion, but the image quality deteriorated with more rapid motion due to motion over the merged undersampled frames and thus over GRAPPA calibration kernels, yielding less accurate GRAPPA weights.

Here, a trajectory is designed specifically for an interleaved self-calibrated through-time GRAPPA approach. The amount of time needed to acquire data at all of the points in the calibration kernel is taken into consideration, in order to minimize the motion over the kernel. We compare the proposed self-calibrated reconstruction to a separately-calibrated reconstruction in digital phantom simulations. Gold-standard cine and real-time data are also acquired in 10 healthy volunteers. Image quality and functional values from the proposed reconstruction are compared to cine datasets.

THEORY

The original implementations of through-time non-Cartesian GRAPPA[14,17] used a fixed undersampling pattern for accelerated data and linear arm ordering for calibration data (Figure 1, left). With linear arm ordering, neighboring points in k-space are acquired close to each other in time, and the time needed to acquire data at all of the points in a calibration kernel is short.

Author Manuscript

In this work, we define a GRAPPA calibration "kernel duration" as an indirect metric of the motion that occurs over the kernel. It is defined as the time that elapses during the collection of all of the data points that are part of a single calibration kernel (Figure 2). Ideally, the underlying object would be approximately stationary while acquiring data in a kernel. The short kernel duration in separately-calibrated GRAPPA helps enforce this.

In the proposed self-calibrated scheme, undersampled data are acquired in an interleaved manner and consecutive frames are merged to form calibration frames (Figure 1, right). This scheme means that neighboring points in k-space are acquired farther apart in time, and the kernel duration must be carefully considered (Figure 2, bottom left).

The design requirement for a short kernel duration led to investigation of using spiral trajectories with longer readouts than previously used for through-time GRAPPA. Longer trajectories have more efficient k-space coverage than shorter ones, and it was hypothesized that a more efficient trajectory could be used to reduce the number of arms needed to sample k-space, thereby reducing the kernel duration and improving the GRAPPA reconstruction.

To further reduce the kernel duration, when forming the calibration kernel, source and target arms could be selected from "forward" or "backward" in time such that source/target pairings were as close as possible in time (Figure 2, bottom right).

METHODS

Trajectory design

Uniform-density spiral trajectories were designed[20] to meet recommended spatiotemporal resolutions for LV evaluation[21,22]. Trajectories were prepared with 300x300mm^2 field-of-view and 2.08x2.08mm^2 in-plane resolution, and with zeroth and first moment gradient balancing for use in a balanced steady-state free precession (bSSFP) sequence. Maximum gradient strength and slew rate were limited to 24mT/m and 170T/m/s, respectively.

Author Manuscript

An initial trajectory with 48 arms as in the original through-time spiral GRAPPA work[17] was designed. The number of arms was then varied from 50 to 3. Preliminary testing[23,24] suggested that acceleration factors of 8 or lower and TRs less than approximately 10ms may yield acceptable image quality. Simulations of trajectories that met these specifications were performed, and those that resulted in visually similar image quality to the separately-calibrated reconstruction were tested in vivo for initial qualitative assessment. This process was iterated until one trajectory was selected for more extensive simulation and in vivo testing.

Digital cardiac phantom simulations

Candidate trajectories were tested using a digital cardiac phantom. In order to realistically simulate motion over a scan, each arm of k-space was sampled from a different image frame, with realistic cardiac and respiratory motion occurring between subsequent TRs. For example, if the accelerated scan had four spiral arms, the arms were sampled from four slightly different images, with motion corresponding to one trajectory-specific TR between each image. The image domain average of the four images was used as the ground truth image. Coil sensitivities derived from a cardiac scan in a healthy volunteer using a 30 channel receiver array were applied to the images prior to conversion to spiral k-space.

Two spiral arm orderings were simulated for accelerated acquisitions: an interleaved arm ordering with an acceleration factor that would enable real-time imaging with temporal resolutions of <45ms, and a fixed arm ordering with the same acceleration factor. A separate, fully-sampled calibration dataset using the same trajectory with linear arm ordering was also simulated.

Undersampled data were reconstructed using the proposed self-calibrated through-time spiral GRAPPA, conventional separately-calibrated through-time spiral GRAPPA, and a sliding window reconstruction (no parallel imaging). The GRAPPA kernel size was fixed to 3 x 2 in the readout and projection directions, as suggested in the original through-time spiral GRAPPA method[17]. Both GRAPPA reconstructions used 80 calibration frames.

Author Manuscript

Reconstruction quality was assessed using structural similarity index (SSIM) and mean normalized root mean square error (RMSE). Both metrics were calculated over 100 accelerated frames, and in each accelerated frame to examine variations over simulated motion.

One trajectory was selected for testing in vivo. For this trajectory, additional simulations were performed over a sweep of cardiac and respiratory rates to evaluate robustness to motion. Cardiac motion was varied from 60-120 beats/minute, and respiration was varied from 12-20 breaths/minute.

In vivo scanning

The trajectory selected for in vivo testing has a TR=8.18ms, and requires 12 arms to fully-sample k-space; data collected at R=3 (4/12 arms) provide a temporal resolution of 32.72ms/cardiac phase.

Data were acquired in 10 healthy volunteers according to an IRB-approved protocol on a 1.5T scanner (Sola, Siemens Healthineers). The spiral multi-slice bSSFP sequence had the following parameters: 8.18/0.93ms TR/TE; 300x300mm^2 field-of-view; 2.08x2.08mm^2 in-plane resolution; 8mm slice thickness; 11-14 slices/stack; 20-25% slice gap; 58°-70° flip angle. Data for each slice were acquired sequentially without pauses, while free-breathing and without ECG gating. 180 undersampled frames were collected in 5.89s/slice, yielding 60 fully-sampled frames for the self-calibrated reconstruction. The total time to acquire a 12-slice stack was 71s.

For comparison, gold-standard breath-held, ECG-gated Cartesian cine scans were collected. Default imaging parameters were used for more accurate comparison to clinical protocols. The parameter ranges were: 255x340mm^2 to 392x396mm^2 field-of-view; 1.52x1.52mm^2 to 1.77x1.77mm^2 in-plane resolution; 8mm slice thickness; 12-14 slices/stack; 20-25% slice gap; 51°-67° flip angle. Depending on the volunteer's heart rate, 11-25 cardiac phases were acquired with 23-52 ms/phase temporal resolution.

Spiral image reconstructions were performed in MATLAB using the proposed self-calibrated through-time spiral GRAPPA method. After reconstruction of the 180 accelerated frames, the

last 4s of data (122 frames) were evaluated. Cartesian cine data were evaluated using vendor-reconstructed images.

Ejection fraction calculation and image quality rating

Images were analyzed in the standard software used at our institution (Medis Suite MR, Medis Medical Imaging). Images were shown to one cardiothoracic radiologist, who performed segmentation and evaluated image quality. The left ventricular endocardium was segmented at end diastole (ED) and end systole (ES) in each slice, and ESV, EDV, and EF were calculated. Although spiral datasets covered multiple heartbeats, the radiologist selected one ED and one ES frame at each slice.

Image quality was rated on a 5-point Likert scale (1=non-diagnostic, 2=poor, 3=average, 4=good, 5=excellent) for the following aspects: level of artifacts, blood-myocardium contrast, sharpness of endocardial border, temporal dynamics of the papillary muscles, and temporal dynamics of the left ventricular wall, as in[18].

For both the segmentation and image quality evaluations, the 20 Cartesian and spiral datasets were presented in random order.

Statistical analyses

The means and standard deviations of ESV, EDV, and EF values for each imaging condition (gold-standard Cartesian and proposed self-calibrated spiral) over the 10 volunteers were calculated. Bland Altman plots[25] and paired t-tests comparing the methods were prepared.

Image quality ratings were pooled over volunteers, yielding 10 ratings for each aspect. Means and standard deviations were calculated for each image set. The gold standard and proposed methods were compared using two-sided Wilcoxon signed-rank tests, with the null hypothesis that the median difference between the two methods is zero. All analyses were performed in MATLAB.

RESULTS

Author Manuscript

Author Manuscript

Figure 3 and Table S1 show a subset of trajectories tested to illustrate trade-offs between different parameters. The first trajectory uses three arms to fully sample k-space, leading to a TR=24.58ms. At R=3, one arm is used to sample each accelerated frame. The GRAPPA calibration kernel duration is the same for both the separate- and self-calibrating schemes because undersampled data are acquired in the same pattern used to acquire linearly-ordered, separate calibration data. The self-calibrating scheme (RMSE=10.1, SSIM=0.979) performs slightly better than the separate calibration for this trajectory (RMSE=13.8, SSIM=0.958). A contrasting trajectory uses 50 arms to fully sample k-space. The TR=4.17ms, and at R=5, the kernel durations are 20.85ms and 87.57ms for the separate- and self-calibrating schemes, respectively. In this case, the separately-calibrated reconstruction (RMSE=10.1, SSIM=0.967) performs better than the self-calibrated reconstruction (RMSE=20.7, SSIM=0.920). Trajectories with intermediate numbers of arms (12, 15, and 24) were also tested. Of these, the 12-arm trajectory had the shortest self-calibrated kernel duration (kernel duration=40.9ms, RMSE=13.0, SSIM=0.958). For all trajectories, both GRAPPA reconstructions performed better than the sliding window reconstruction in terms of RMSE and SSIM.

Visual differences in image quality of the different trajectories are shown in Figure 4 and Figure S1. Difference images from the ground truth show that as the number of arms and kernel duration increase, the self-calibrated reconstruction begins to exhibit errors at the edges of the heart walls and swirling artifacts in the blood pool (Figure 4). Temporal profiles (Figure S1) also show increasing differences in the self-calibrated reconstruction from ground truth as the number of arms increases. The separately-calibrated reconstruction showed less dependence on the number of arms in terms of RMSE and SSIM (Figure 3), and the image quality appears more consistent visually over the trajectories (Figure 4, Figure S1). Plots of RMSE and SSIM at each accelerated frame (Figure S1) show that the self-calibrated reconstruction has a slightly wider range in both metrics compared to the separately-calibrated reconstruction, indicating more variation in image quality over time. Compared to the sliding window reconstruction, both GRAPPA reconstructions show better image quality.

Effects of different levels of simulated cardiac and respiratory motion are shown in Figures S2-S4. The image quality of all three reconstructions deteriorates as the simulated heart and

Author Manuscript

respiratory rates increase (Figure S2). However, the separately-calibrated GRAPPA reconstruction shows the least sensitivity to motion (60bpm: RMSE=8.25, SSIM=0.977; 120bpm: RMSE=8.77, SSIM=0.972), while the sliding window reconstruction shows the most sensitivity (60bpm: RMSE=29.0, SSIM=0.905; 120bpm: RMSE=40.2, SSIM=0.845). The self-calibrated GRAPPA reconstruction shows an intermediate amount of sensitivity (60bpm: RMSE=9.69, SSIM=0.973; 120bpm: RMSE=15.5, SSIM=0.944).

Figure 5 shows frames at ED and ES from the gold-standard Cartesian cine scan and the proposed self-calibrated spiral GRAPPA method at a stack of slices in one volunteer. For this volunteer, the spiral images had a slightly higher average image quality rating (average=3.8) than the Cartesian images (average=3.2). The two methods yielded similar functional values (spiral: ESV=44.7mL, EDV=104mL, EF=57.0%; Cartesian: ESV=46.3mL, EDV=115mL, EF=59.9%).

Figure 6 shows images from a second volunteer at basal, mid-ventricular, and apical slices. The average image quality of the Cartesian images (average=4.8) was higher than the spiral images (average=3.8). Functional values were also similar (spiral: ESV=50.2mL, EDV=116mL, EF=56.8%; Cartesian: ESV=46.61mL, EDV=117mL, EF=60.2%).

Figure 7 shows a set of images from a third volunteer, in which banding artifacts were seen over the ventricular wall in the spiral images. The average image quality of the Cartesian scans was 3.6, while the spiral scans were rated 3.2. However, the functional values were similar between the two methods (spiral: ESV=58.7mL, EDV=151mL, EF=61.1%; Cartesian: ESV=62.0mL, EDV=149mL, EF=58.5%). Videos corresponding to Figures 5-7 are available in the supporting material.

Figure 8 shows Bland-Altman comparisons between the two methods for the three functional values. The mean biases ([95% limits of agreement]) were 0.036mL ([-10.6, 10.7]), 1.83mL ([-29.8, 33.5]), and 0.167% ([-9.99, 10.3]) for ESV, EDV, and EF, respectively. All volunteers fell within the limits of agreement for the three values, except for EDV of one volunteer.

Author Manuscript

Table 1 summarizes the Bland-Altman statistics, and shows absolute differences and paired t-test p-values comparing the gold standard and proposed methods. Mean absolute differences in ESV, EDV, and EF were 4.60mL, 11.1mL, and 4.22%, while maximum absolute differences were 9.04mL, 34.2mL, and 10.1%, respectively. The p-values for ESV, EDV, and EF were 0.984, 0.728, and 0.921, respectively. These results indicate that functional values calculated using the two methods are not statistically significantly different ($p<0.05$).

A summary of the image quality ratings is given in Table 2. The Cartesian scans had higher ratings for all five aspects, and ratings were statistically significantly different for the level of artifacts and the blood-myocardium contrast. However, the average rating for the spiral images was greater than 3 (average) for all aspects except the level of artifacts, for which the average rating was 2.8. Figure S5 shows a bar graph of the ratings for a more detailed breakdown.

DISCUSSION

This work presents a method for self-calibrated through-time spiral GRAPPA that removes the need to acquire separate calibration data. Undersampled data are acquired with interleaved arm ordering, and consecutive frames are merged together to form calibration data. The GRAPPA weights are then used to reconstruct individual undersampled frames. Real-time images generated with this method can be used to calculate left ventricular functional values in a single rapid, free-breathing, ungated scan.

One focus of this work was the design of a spiral trajectory with better robustness to motion after merging undersampled frames to form calibration data. To this end, we defined a "kernel duration" metric as the time that elapses while acquiring all of the data points that make up a GRAPPA calibration kernel. Spiral trajectories with short TRs require more arms to fully sample k-space, and higher acceleration factors are needed to reach recommended temporal resolutions. The higher acceleration factor may lead to a longer kernel duration that starts to violate the assumption that the underlying object is stationary while data in the kernel are acquired. In this case, the GRAPPA weights may not reflect the true coil sensitivity information, resulting in poor image quality. This effect was observed in simulations of a 50-arm interleaved trajectory with a kernel duration of 87.57ms at R=5. Artifacts resembled those in the sliding window

reconstruction, suggesting they may be due to motion across arms used together in a calibration kernel. Longer trajectories with lower acceleration factors had better image quality due to the shorter kernel durations.

Simulations were also performed to compare the proposed self-calibrated reconstruction to separately-calibrated GRAPPA. While the self-calibrating approach reduced the total scan time for a short-axis stack from 142s to 71s, the separately-calibrated reconstructions demonstrated lower RMSE values. This may be expected because the kernel duration is shorter when data are acquired with linear arm ordering compared to interleaved ordering. The separately-calibrated approach may be beneficial if the time is available and the patient is compliant. However, despite the potential for reduced image quality, the self-calibrated approach still led to functional values in agreement with the gold-standard.

Several groups have proposed self-calibrated, non-Cartesian GRAPPA methods. Two early methods multiplied undersampled images by a support mask[26] or coil sensitivities[27], effectively convolving undersampled k-space with a filter to approximate fully-sampled data. However, one method[26] noted residual artifacts when R is high, and the second[27] described an upper limit on R because a fully-sampled center of k-space is needed. Therefore, these methods may not be suitable for real-time cardiac imaging. Others use the geometric patterns of propeller and radial trajectories to overlap undersampled data into fully-sampled regions[28], interpolate GRAPPA weights[29], or accumulate calibration data over undersampled k-space[30]. However, these methods cannot be easily adapted to spiral trajectories. A recent method uses the Fourier transform phase shift property on fully-sampled Cartesian data to estimate GRAPPA kernels for arbitrary trajectories[31]. It is demonstrated with fMRI datasets, and it is unclear if it would perform as well at the temporal resolutions needed for cardiac imaging. Another method[32] merges interleaved, undersampled acquisitions into fully-sampled datasets that can be re-sampled at desired non-Cartesian kernels. However, it was tested on breath-held, cine cardiac images.

Unlike some of these previous works, the proposed method is demonstrated for prospectively undersampled, free-breathing and ungated cardiac imaging. One previous method for free-breathing, ungated cardiac imaging achieves high spatiotemporal resolutions of up to

Author Manuscript

1.3x1.3mm^2 and 38ms/frame[30]. However, it relied on the geometry of radial trajectories, and acceleration factors of 6-16 were needed for these resolutions. Here, a specially designed interleaved spiral trajectory is used to reach clinically relevant resolutions at R=3.

In addition to GRAPPA-type methods, other parallel imaging methods such as CG-SENSE have been used for real-time cardiac imaging using undersampled, non-Cartesian acquisitions[33]. Compared to CG-SENSE, through-time GRAPPA is a non-iterative approach, and it does not require coil sensitivity maps to be calculated. However, future work may directly compare the proposed method to other types of reconstructions such as CG-SENSE in terms of image quality and practical implementation. While the proposed method is not iterative, it does require calculation of R times more GRAPPA weights than conventional separately-calibrated GRAPPA due to the interleaved acquisition pattern. In this work we did not attempt to optimize the reconstruction time, and parallelized implementations using GPUs could be explored to speed it up, similar to fast implementations of the CG-SENSE algorithm[34].

Results in healthy volunteers showed that functional values calculated using the proposed self-calibrated spiral GRAPPA method were not statistically significantly different from the gold standard. Pellikka et al[35] suggest that when comparing different imaging modalities to calculate EF, an absolute difference of <5% may be considered in agreement. In this work, the largest absolute difference was 10.1%, and the mean absolute difference was 4.22%. Bland-Altman comparisons showed small biases for the three functional values, and all results except one fell within the limits of agreement. However, the limits are wider than those reported in prior works using through-time non-Cartesian GRAPPA for LV evaluation[16,18]. One possible reason is that datasets were presented in random order to the radiologist, and the number of slices selected from each stack for LV coverage was not consistent between the gold-standard and proposed scans for each volunteer. For example, for the volunteer with the largest difference in EF, the number of slices in diastole differed by 2, while the number of slices in systole was the same. Because scans were prepared with the same slice positions, thicknesses, and gaps, a difference in the number of slices may cause differences in calculated volumes. Future experiments should include long-axis views to assist the radiologist in selecting slices.

Author Manuscript

Author Manuscript

Five features were rated to compare the image quality of the proposed and gold-standard methods. Ratings were statistically significantly different for two aspects (blood-myocardium contrast, levels of artifacts). However, the only average rating below 3 (average) using the proposed method was for level of artifacts. It is expected that the non-Cartesian sampling, longer TR, and smaller field-of-view of the proposed method may result in different artifacts than the gold-standard. For the three real-time datasets that had ratings of 2 (poor) for the level of artifacts, the primary artifacts were flow artifacts and banding.

The second statistically significantly different feature was the blood-myocardium contrast, although no ratings were below 3 for either method. We did not optimize the flip angle for the spiral design, and flip angles used for real-time scanning with the long TR (58°-70°) were similar to those used for Cartesian scanning (51°-67°). Future work may optimize the flip angle to improve contrast.

The remaining three image features (sharpness of endocardial border, temporal dynamics of papillary muscles, temporal dynamics of left ventricular wall) had lower, but not statistically significantly different, ratings for the real-time images. The temporal dynamics of the papillary muscles and the ventricular wall had the most similar ratings between the two methods, possibly reflecting the similar temporal resolutions of the self-calibrated (32.72ms/phase) and gold-standard (23-52ms/phase) methods. One strength of the proposed method is that comparable temporal resolution can be achieved in a real-time acquisition, without combining data from multiple heartbeats.

These results suggest that the gold-standard method may result in better image quality in patients who are able to breath-hold and who have regular heart rhythms. Other studies comparing real-time and gold-standard cardiac imaging have also reported inferior image quality from real-time images[11,12,16]. Future work will assess whether the method proposed here provides acceptable image quality in patients who are unable to comply with the gold-standard scans. For these patients, the proposed method may provide a fast free-breathing, ungated alternative to obtain functional values.

Author Manuscript

This initial study was performed in healthy volunteers. Other studies testing real-time methods in patient populations have shown promising results[11–13,16,33]. Future evaluation of the proposed method in patients may test its performance in a wider range of functional values and for various cardiac characteristics, such as presence of arrhythmias, wall motion abnormalities, or disease, to understand the clinical utility of the method.

CONCLUSION

A method for self-calibrated through-time spiral GRAPPA was presented. Undersampled data were acquired using a specially designed spiral trajectory with interleaved arm ordering, and consecutive frames were merged to form fully-sampled calibration data. The resulting GRAPPA weights were then used to reconstruct the undersampled frames, eliminating the need for a separate calibration scan. This method enables real-time imaging of 12 slices for left ventricular coverage in 71 seconds of free-breathing, ungated scanning. The temporal resolution is 32.72ms/cardiac phase, with a 2.08x2.08mm^2 spatial resolution, 300x300mm^2 field-of-view, and 8mm slice thickness. Functional values calculated using the proposed self-calibrated method and the gold-standard method were not statistically significantly different. Image quality ratings for the real-time images were lower than for the gold-standard method, although only one image aspect (level of artifact) had an average rating less than 3 (average). These results indicate that real-time imaging with self-calibrated spiral GRAPPA may be an option for patients who are unable to breath-hold or who have irregular heart rates.

ACKNOWLEDGEMENTS

This work was supported by the NIH grants: R01HL153034, F30CA239355, and T32GM07250, and by the NSF grant: 1563805.

Author Manuscript

REFERENCES

1. Grothues F, Smith GC, Moon JCC, et al. Comparison of interstudy reproducibility of cardiovascular magnetic resonance with two-dimensional echocardiography in normal subjects and in patients with heart failure or left ventricular hypertrophy. *Am J Cardiol*. 2002;90(1):29-34. doi:10.1016/S0002-9149(02)02381-0
2. Patel MR, White RD, Abbara S, et al. 2013 ACCF/ACR/ASE/ASNC/SCCT/SCMR appropriate utilization of cardiovascular imaging in heart failure: A joint report of the American college of radiology appropriateness criteria committee and the American college of cardiology foundation appropriate use c. *J Am Coll Cardiol*. 2013;61(21):2207-2231. doi:10.1016/j.jacc.2013.02.005
3. Bustin A, Fuin N, Botnar RM, Prieto C. From Compressed-Sensing to Artificial Intelligence-Based Cardiac MRI Reconstruction. *Front Cardiovasc Med*. 2020;7(February):1-19. doi:10.3389/fcvm.2020.00017
4. Wang X, Uecker M, Feng L. Fast Real-Time Cardiac MRI: a Review of Current Techniques and Future Directions. *Investig Magn Reson Imaging*. 2021;25(4):252. doi:10.13104/imri.2021.25.4.252
5. Nayak KS, Lim Y, Campbell-Washburn AE, Steeden J. Real-Time Magnetic Resonance Imaging. *J Magn Reson Imaging*. 2020:1-19. doi:10.1002/jmri.27411
6. Breuer FA, Kellman P, Griswold MA, Jakob PM. Dynamic autocalibrated parallel imaging using temporal GRAPPA (TGRAPPA). *Magn Reson Med*. 2005;53(4):981-985. doi:10.1002/mrm.20430
7. Kellman P, Epstein FH, Mcveigh ER. Adaptive Sensitivity Encoding Incorporating Temporal Filtering (TSENSE). *Magn Reson Med*. 2001;45:846-852. doi:https://doi.org/10.1002/mrm.1113
8. Pruessmann KP, Weiger M, Börnert P, Boesiger P. Advances in sensitivity encoding with arbitrary k-space trajectories. *Magn Reson Med*. 2001;46(4):638-651. doi:10.1002/mrm.1241
9. Tsao J, Boesiger P, Pruessmann KP. k-t BLAST and k-t SENSE: Dynamic MRI With High Frame Rate Exploiting Spatiotemporal Correlations. *Magn Reson Med*. 2003;50:1031-1042. doi:10.1002/mrm.10611
10. Uecker M, Zhang S, Voit D, Karaus A, Merboldt KD, Frahm J. Real-time MRI at a

Author Manuscript

resolution of 20 ms. *NMR Biomed*. 2010;23(8):986-994. doi:10.1002/nbm.1585

11. Voit D, Zhang S, Unterberg-Buchwald C, Sohns JM, Lotz J, Frahm J. Real-time cardiovascular magnetic resonance at 1.5 T using balanced SSFP and 40 ms resolution. *J Cardiovasc Magn Reson*. 2013;15(1):1-8. doi:10.1186/1532-429X-15-79
12. Feng L, Srichai MB, Lim RP, et al. Highly accelerated real-time cardiac cine MRI using k-t SPARSE-SENSE. *Magn Reson Med*. 2013;70(1):64-74. doi:10.1002/mrm.24440
13. Hauptmann A, Arridge S, Lucka F, Muthurangu V, Steeden JA. Real-time cardiovascular MR with spatio-temporal artifact suppression using deep learning–proof of concept in congenital heart disease. *Magn Reson Med*. 2018;81(2):1143-1156. doi:10.1002/mrm.27480
14. Seiberlich N, Ehses P, Duerk J, Gilkeson R, Griswold M. Improved radial GRAPPA calibration for real-time free-breathing cardiac imaging. *Magn Reson Med*. 2011;65(2):492-505. doi:10.1002/mrm.22618
15. Saybasili H, Herzka DA, Seiberlich N, Griswold MA. Real-time imaging with radial GRAPPA: Implementation on a heterogeneous architecture for low-latency reconstructions. *Magn Reson Imaging*. 2014;32(6):747-758. doi:10.1016/j.mri.2014.02.022
16. Aandal G, Nadig V, Yeh V, et al. Evaluation of left ventricular ejection fraction using through-time radial GRAPPA. *J Cardiovasc Magn Reson*. 2014;16(79):1-13.
17. Seiberlich N, Lee G, Ehses P, Duerk JL, Gilkeson R, Griswold M. Improved temporal resolution in cardiac imaging using through-time spiral GRAPPA. *Magn Reson Med*. 2011;66(6):1682-1688. doi:10.1002/mrm.22952
18. Barkauskas KJ, Rajiah P, Ashwath R, et al. Quantification of left ventricular functional parameter values using 3D spiral bSSFP and through-time non-Cartesian GRAPPA. *J Cardiovasc Magn Reson*. 2014;16(65):1-13.
19. Hamilton JI, Wright KL, Griswold MA, Seiberlich N. Self-Calibrating Interleaved Reconstruction for Through-Time Non-Cartesian GRAPPA. In: *Proceedings of the 13th Annual Meeting of the International Society for Magnetic Resonance in Medicine*. Salt Lake City; 2013:3836.
20. Hargreaves B. Variable-Density Spiral Design Functions. http://mrsrl.stanford.edu/~brian/vdspiral/.

Author Manuscript

21. Kramer CM, Barkhausen J, Bucciarelli-Ducci C, Flamm SD, Kim RJ, Nagel E. Standardized cardiovascular magnetic resonance imaging (CMR) protocols: 2020 update. *J Cardiovasc Magn Reson*. 2020;22(1):1-18. doi:10.1186/s12968-020-00607-1
22. Fratz S, Chung T, Greil GF, et al. Guidelines and protocols for cardiovascular magnetic resonance in children and adults with congenital heart disease : SCMR expert consensus group on congenital heart disease. *J Cardiovasc Magn Reson*. 2013;15(51):1-26.
23. Franson D, Hamilton J, Griswold M, Seiberlich N. Self-calibrating through-time spiral GRAPPA for flexible real-time imaging. In: *Proceedings of the 27th Meeting of the International Society for Magnetic Resonance in Medicine*. Montreal; 2019:1184.
24. Franson D, Ahad J, Liu Y, Fyrdahl A, Seiberlich N. Self-calibrated through-time spiral GRAPPA for real-time, free-breathing evaluation of left ventricular function. In: *Proceedings of the 31st Annual Meeting of the ISMRM*. London; 2022:2615.
25. Bland JM, Altman DG. Statistical methods for assessing agreement between two methods of clinical measurement. *Lancet*. 1986;327(8476):307-310. doi:https://doi.org/10.1016/S0140-6736(86)90837-8
26. Huang F, Vijayakumar S, Li Y, Hertel S, Reza S, Duensing GR. Self-calibration method for radial GRAPPA/k-t GRAPPA. *Magn Reson Med*. 2007;57(6):1075-1085. doi:10.1002/mrm.21233
27. Arunachalam A, Samsonov A, Block WF. Self-Calibrated GRAPPA method for 2D and 3D radial data. *Magn Reson Med*. 2007;57(5):931-938. doi:10.1002/mrm.21223
28. Skare S, Newbould RD, Nordell A, Holdsworth SJ, Bammer R. An auto-calibrated, angularly continuous, two-dimensional GRAPPA kernel for propeller trajectories. *Magn Reson Med*. 2008;60(6):1457-1465. doi:10.1002/mrm.21788
29. Codella NCF, Spincemaille P, Prince M, Wang Y. A radial self-calibrated (RASCAL) generalized autocalibrating partially parallel acquisition (GRAPPA) method using weight interpolation. *NMR Biomed*. 2011;24(7):844-854. doi:10.1002/nbm.1630
30. Sayin O, Saybasili H, Zviman MM, et al. Real-time free-breathing cardiac imaging with self-calibrated through-time radial GRAPPA. *Magn Reson Med*. 2017;77(1):250-264. doi:10.1002/mrm.26112
31. Luo T, Noll DC, Fessler JA, Nielsen JF. A GRAPPA algorithm for arbitrary 2D/3D non-Cartesian sampling trajectories with rapid calibration. *Magn Reson Med*.

2019;82(3):1101-1112. doi:10.1002/mrm.27801

32. Chieh SW, Kaveh M, Akçakaya M, Moeller S. Self-calibrated interpolation of non-Cartesian data with GRAPPA in parallel imaging. *Magn Reson Med*. 2020;83(5):1837-1850. doi:10.1002/mrm.28033
33. Contijoch F, Witschey WRT, Rogers K, et al. User-initialized active contour segmentation and golden-angle real-time cardiovascular magnetic resonance enable accurate assessment of LV function in patients with sinus rhythm and arrhythmias. *J Cardiovasc Magn Reson*. 2015;17(1):1-12. doi:10.1186/s12968-015-0146-9
34. Sorensen TS, Prieto C, Atkinson D, Hansen MS, Schaeffter T. GPU accelerated iterative SENSE reconstruction of radial phase encoded whole-heart MRI. In: *Proc. Intl. Soc. Mag. Reson. Med. 10*. Vol 18. ; 2010. doi:10.1109/TMI.2009.2027118.Figure
35. Pellikka PA, She L, Holly TA, et al. Variability in Ejection Fraction Measured by Echocardiography, Gated Single-Photon Emission Computed Tomography, and Cardiac Magnetic Resonance in Patients with Coronary Artery Disease and Left Ventricular Dysfunction. *JAMA Netw Open*. 2018;1(4). doi:10.1001/jamanetworkopen.2018.1456

Author Manuscript

Author Manuscript

FIGURE CAPTIONS

Figure 1: Schematic of separately-calibrated and the proposed self-calibrated through-time spiral GRAPPA acquisition. In the original implementation of through-time spiral GRAPPA, fully-sampled calibration data are acquired in a separate scan from the accelerated data (left). In the proposed self-calibrated implementation, accelerated data are acquired in an interleaved manner, and consecutive frames are merged to form fully-sampled calibration data (right).

Figure 2: GRAPPA calibration kernel duration. The calibration kernel duration is defined as the amount of time that elapses while acquiring calibration data over all of the points in the GRAPPA kernel. (Top) Source and target points in an example GRAPPA kernel. Source points are blue, target point is red. Open points/gray arm lines are uncollected, and filled points/black arm lines are collected. (Middle) Using linear arm ordering, neighboring shots in k-space are acquired consecutively in time. In this example using a TR=8.18ms and R=3, the kernel duration is 3 TRs, or 24.54ms. (Bottom left) Using interleaved arm ordering, neighboring arms are not acquired consecutively. Instead, all of the shots for one undersampled frame are acquired before moving to the next undersampled frame at the next set of shots. Here, the kernel duration is 8 TRs, or 65.44ms. (Bottom right) This work used a forward/backward GRAPPA kernel to shorten the kernel duration. Source and target points to fill a calibration kernel could be taken from any set of neighboring undersampled frames, not just those that are acquired after the first source point in time. Undersampled frames 1, 2, and 3 are the three different arm sets in the R=3 interleaved trajectory. In the forward-only kernel, frames 1, 2, and 3 need to be collected to form the calibration kernel. In the forward/backward pattern, prior frame 3 and then frame 1 can be used for a shorter kernel duration. The elapsed time (ET) is the time elapsed since the first point in the kernel was acquired (T = 0).

Figure 3: Comparison of sample trajectories tested in digital phantom simulations. The trajectories differ in the number of arms in the fully-sampled k-space, and thus both the repetition time (TR) and the time elapsed over the GRAPPA calibration kernel in separately and self-calibrated modes. The acceleration factor was chosen such that the temporal resolution per accelerated frame is less than 45ms, as recommended for evaluation of LV structure and

Author Manuscript

function[21,22]. Please see Supporting Information Table 1 for the kernel durations and acceleration factors of these trajectories. RMSE and SSIM values are calculated compared to ground truth images, and are given for the two spiral GRAPPA implementations and a sliding window reconstruction. All simulations were performed for a heart rate of 90 beats per minute and a respiratory rate of 16 breaths per minute.

Figure 4: Sample digital phantom images in diastole, mid-cycle, and systole corresponding to the trajectories in Figure 3. Images from the two spiral GRAPPA implementations and the sliding window reconstruction are given, along with subtraction images compared to the ground truth (x2 scale).

Figure 5: Stack of images in diastole and systole from one volunteer. Images are shown for the gold-standard breath-held, ECG-gated Cartesian scan and the proposed self-calibrated GRAPPA scan. 12 slices were acquired in vivo, but only the 8 required for left ventricular coverage are shown. Images are cropped to better show the heart. For this volunteer, the average image quality rating for the gold-standard scan was 3.2 (blood-myocardium contrast=5, sharpness of endocardial border=3, temporal dynamics of papillary muscles=3, temporal dynamics of ventricular wall=2, level of artifacts=3). The average image quality rating for the self-calibrated GRAPPA scan was 3.8 (blood-myocardium contrast=4, sharpness of endocardial border=3, temporal dynamics of papillary muscles=4, temporal dynamics of ventricular wall=4, level of artifacts=4).

Figure 6: Images from a second volunteer at 3 slice locations (basal, mid-ventricular, apex) in diastole and systole for each imaging condition. The average image quality rating of the Cartesian images was 4.8 (blood-myocardium contrast=5, sharpness of endocardial border=5, temporal dynamics of papillary muscles=5, temporal dynamics of ventricular wall=5, level of artifacts=4). The average rating of the spiral images was 3.8 (blood-myocardium contrast=4, sharpness of endocardial border=4, temporal dynamics of papillary muscles=4, temporal dynamics of ventricular wall=4, level of artifacts=3).

Figure 7: Images from a third volunteer at three slice locations (basal, mid-ventricular, apex) in

diastole and systole for each imaging condition. In this volunteer, banding artifacts (red arrows) were seen in the ventricular wall, which were not seen in the Cartesian scans. The average image quality rating of the Cartesian scans was 3.6 (blood-myocardium contrast=4, sharpness of endocardial border=3, temporal dynamics of papillary muscles=4, temporal dynamics of ventricular wall=3, level of artifacts=4). The average rating for the spiral scan was 3.2 (blood-myocardium contrast=3, sharpness of endocardial border=3, temporal dynamics of papillary muscles=4, temporal dynamics of ventricular wall=4, level of artifacts=2).

Figure 8: Bland-Altman plots comparing functional values from the gold standard (breath-held Cartesian) and proposed (self-calibrating spiral) methods.

Table 1: Comparison of functional values calculated using the proposed self-calibrated spiral GRAPPA method and the gold-standard Cartesian cine. Statistics are given over 10 healthy volunteers.

Table 2: Likert scale ratings of different image quality aspects for each of the imaging methods. Mean ± SD over 10 volunteers are given. Each aspect was rated on a 5 point Likert scale (1: non-diagnostic, 2: poor, 3: average, 4: good, 5: excellent). Note that a lower rating for the level of artifacts indicates worse artifacts. The pWSR level is given between the gold-standard Cartesian and the self-calibrated GRAPPA methods. Asterisked values indicate features that were statistically significantly different ($p < 0.05$).

Supporting Information Table S1: Characteristics of sample trajectories tested in digital phantom simulations.

Supporting Information Figure S1: Temporal profiles over 100 accelerated images corresponding to the trajectories in Figure 3. The line profiles track the position shown in the simulated heart. Subtraction images are scaled by x2. The right two columns plot RMSE and SSIM by frame for each of the reconstructions. For both values, the mean value over all time frames is subtracted from each time frame such that the three reconstructions can be viewed on the same y-axis.

Author Manuscript

Author Manuscript

Supporting Information Figure S2: Effect of cardiac and respiratory motion on the two through-time spiral GRAPPA implementations and a sliding window reconstruction. Digital phantom simulations were performed using the 12-arm trajectory used for in vivo scanning.

Supporting Information Figure S3: Sample digital phantom images in diastole, mid-cycle, and systole corresponding to different motion conditions. Images from the two spiral GRAPPA implementations and the sliding window reconstruction are given, along with subtraction images compared to the ground truth (x2 scale).

Supporting Information Figure S4: Temporal profiles over 100 accelerated images corresponding to different motion conditions. Subtraction images are scaled by x2. The right two columns plot RMSE and SSIM by frame for each of the reconstructions. For both values, the mean value over all time frames is subtracted from each value such that the three reconstructions can be viewed on the same y-axis.

Supporting Information Figure S5: Comparison of Likert scale ratings of different image quality aspects for the gold-standard, ECG-gated and breathheld Cartesian scan (BC) and the proposed real-time, free-breathing spiral scan (FS). Asterisk indicates statistical significance to the $p<0.05$ level in a Wilcoxon signed rank test between the gold standard and proposed methods.

Supporting Information Video S1: Time series corresponding to Figure 5. Images from all phases in a gold-standard breath-held, ECG-gated Cartesian scan at a stack of 8 slices for left ventricular coverage in a healthy volunteer. Images are cropped to better show the heart.

Supporting Information Video S2: Time series corresponding to Figure 5. Images at a stack of 8 slices in a healthy volunteer from 4 seconds of free-breathing, ungated imaging acquired and reconstructed using the proposed self-calibrated spiral GRAPPA method. Note that because data are ungated and acquired slice-by-slice, the cardiac phases are not temporally aligned across the slices. Images are cropped to better show the heart.

Author Manuscript

Supporting Information Video S3: Time series corresponding to Figure 5 and Video S2. To visually compare the proposed self-calibrated and conventional separately-calibrated spiral GRAPPA methods, the same interleaved, undersampled dataset shown in Video S2 was reconstructed using separately-calibrated GRAPPA. GRAPPA weights were calculated using a separate fully-sampled acquisition.

Supporting Information Video S4: Time series corresponding to Figure 6. Images from all phases in a gold-standard breath-held, ECG-gated Cartesian scan at 3 slice locations (basal, mid-ventricular, apex) in a second healthy volunteer.

Supporting Information Video S5: Time series corresponding to Figure 6. Images at 3 slice locations (basal, mid-ventricular, apex) in a second healthy volunteer from 4 seconds of free-breathing, ungated imaging acquired and reconstructed using the proposed self-calibrated spiral GRAPPA method.

Supporting Information Video S6: Time series corresponding to Figure 6 and Video S5. To visually compare the proposed self-calibrated and conventional separately-calibrated spiral GRAPPA methods, the same interleaved, undersampled dataset shown in Video S5 was reconstructed using separately-calibrated GRAPPA. GRAPPA weights were calculated using a separate fully-sampled acquisition.

Supporting Information Video S7: Time series corresponding to Figure 7. Images from all phases in a gold-standard breath-held, ECG-gated Cartesian scan at 3 slice locations (basal, mid-ventricular, apex) in a third healthy volunteer.

Supporting Information Video S8: Time series corresponding to Figure 7. Images at 3 slice locations (basal, mid-ventricular, apex) in a third healthy volunteer from 4 seconds of free-breathing, ungated imaging acquired and reconstructed using the proposed self-calibrated spiral GRAPPA method. In this volunteer, banding artifacts were seen in the ventricular wall of the spiral scans, which were not seen in the Cartesian scans.

Author Manuscript

Supporting Information Video S9: Time series corresponding to Figure 7 and Video S8. To visually compare the proposed self-calibrated and conventional separately-calibrated spiral GRAPPA methods, the same interleaved, undersampled dataset shown in Video S8 was reconstructed using separately-calibrated GRAPPA. GRAPPA weights were calculated using a separate fully-sampled acquisition.

	Bland-Altman statistics			**Absolute differences**		**Paired t-test**
Functional metric	Mean bias	Lower limit of agreement (-1.96 SD)	Upper limit of agreement (+1.96 SD)	Mean absolute difference	Maximum absolute difference	p-value
ESV (mL)	0.036	-10.6	10.7	4.60	9.04	0.984
EDV (mL)	1.83	-29.8	33.5	11.1	34.2	0.728
EF (%)	0.167	-9.99	10.3	4.22	10.1	0.921

Table 1: Comparison of functional values calculated using the proposed self-calibrated spiral GRAPPA method and the gold-standard Cartesian cine. Statistics are given over 10 healthy volunteers.

	Cartesian gold standard	**Self-calibrated GRAPPA**	**pWSR**
Level of artifacts	4.1 ± 0.57	2.8 ± 0.63	0.016*
Blood-myocardium contrast	4.6 ± 0.70	3.5 ± 0.53	0.0039*
Sharpness of endocardial border	3.9 ± 0.88	3.1 ± 0.74	0.078

Temporal dynamics of the papillary muscles	4.4 ± 0.84	3.7 ± 0.95	0.17
Temporal dynamics of the left ventricular wall	4.1 ± 1.1	3.8 ± 0.79	0.55

Table 2: Likert scale ratings of different image quality aspects for each of the imaging methods. Mean ± SD over 10 volunteers are given. Each aspect was rated on a 5 point Likert scale (1: non-diagnostic, 2: poor, 3: average, 4: good, 5: excellent). Note that a lower rating for the level of artifacts indicates worse artifacts. The pWSR level is given between the gold-standard Cartesian and the self-calibrated GRAPPA methods. Asterisked values indicate features that were statistically significantly different ($p < 0.05$).

Author Manuscript

Author Manuscript

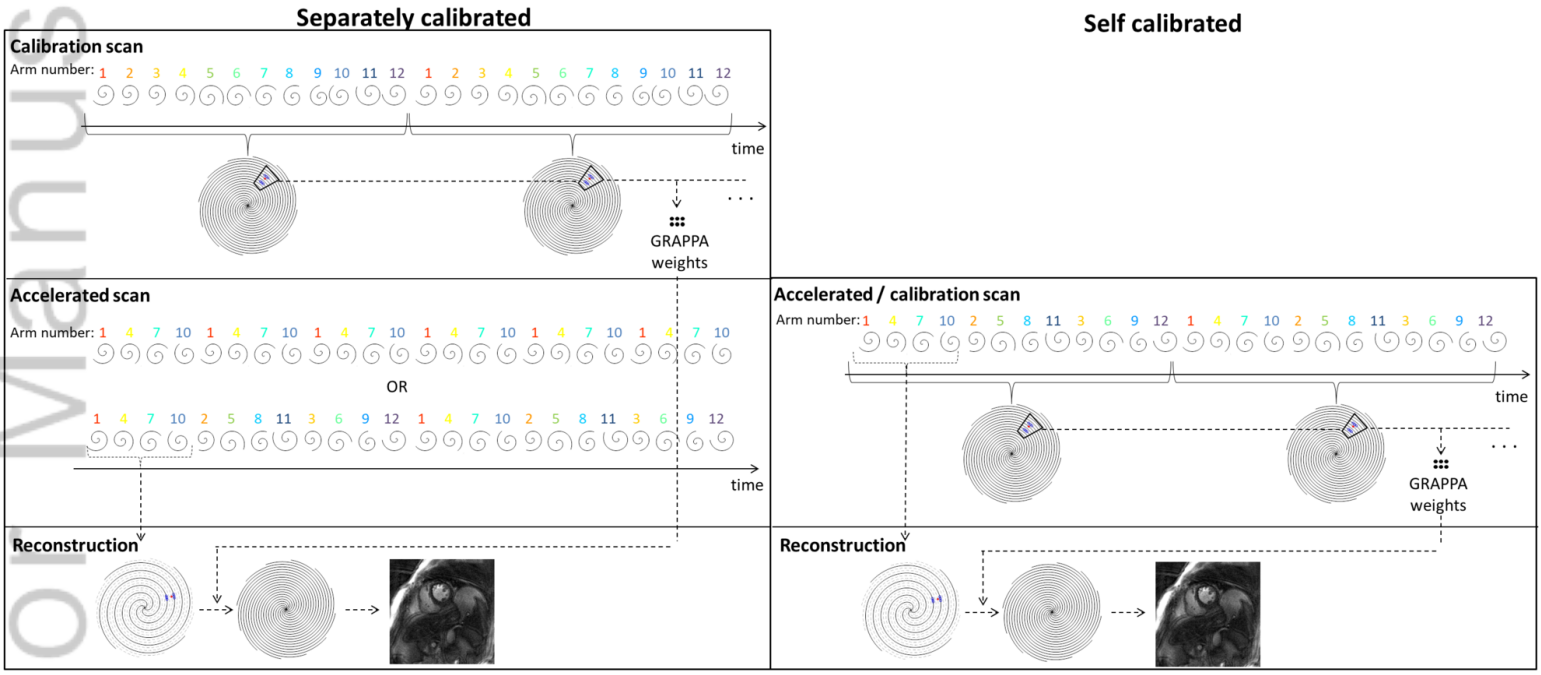

MRM_29462_Figure1.tif

Author Manuscript

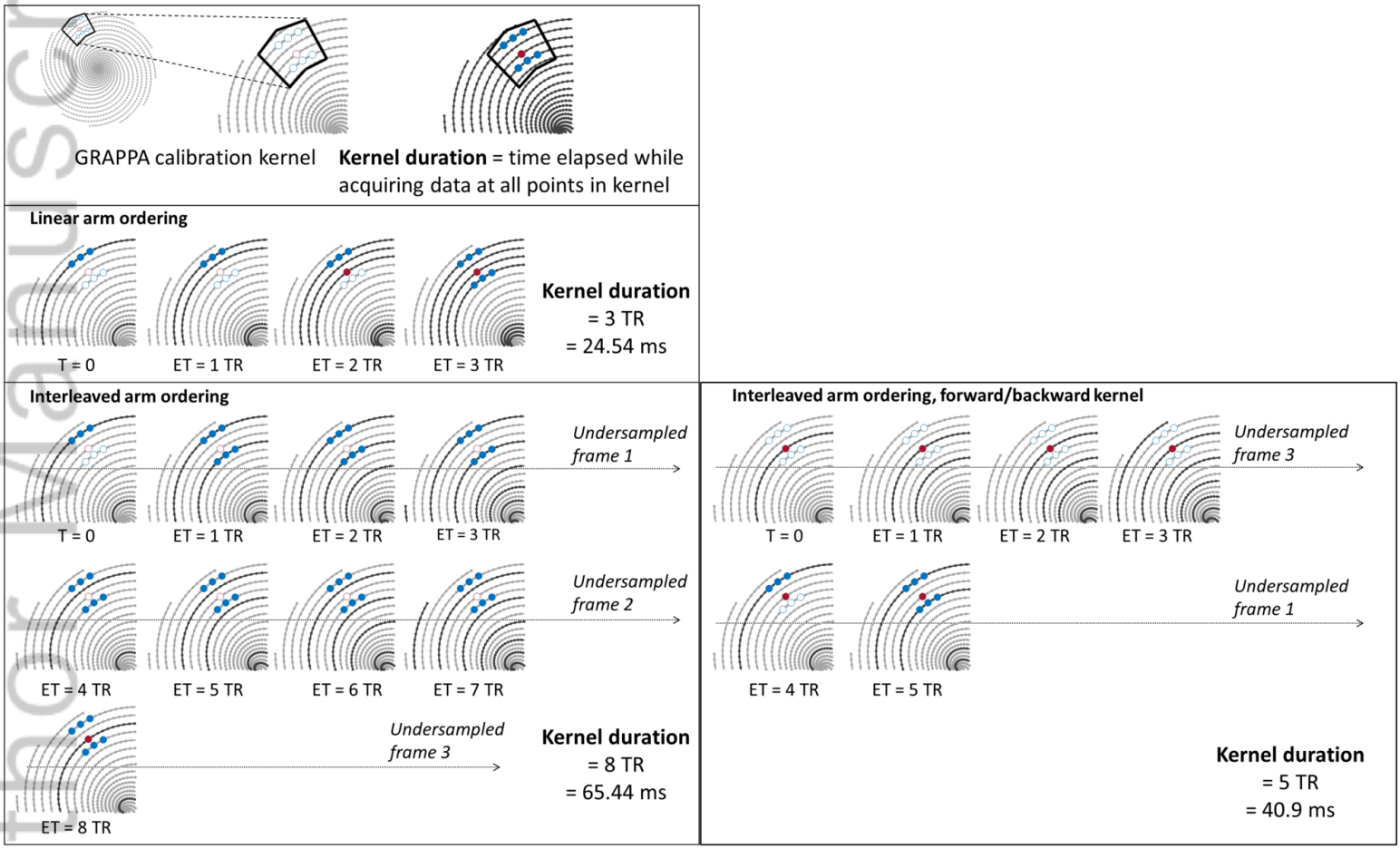

MRM_29462_Figure2.tif

Author Manuscript

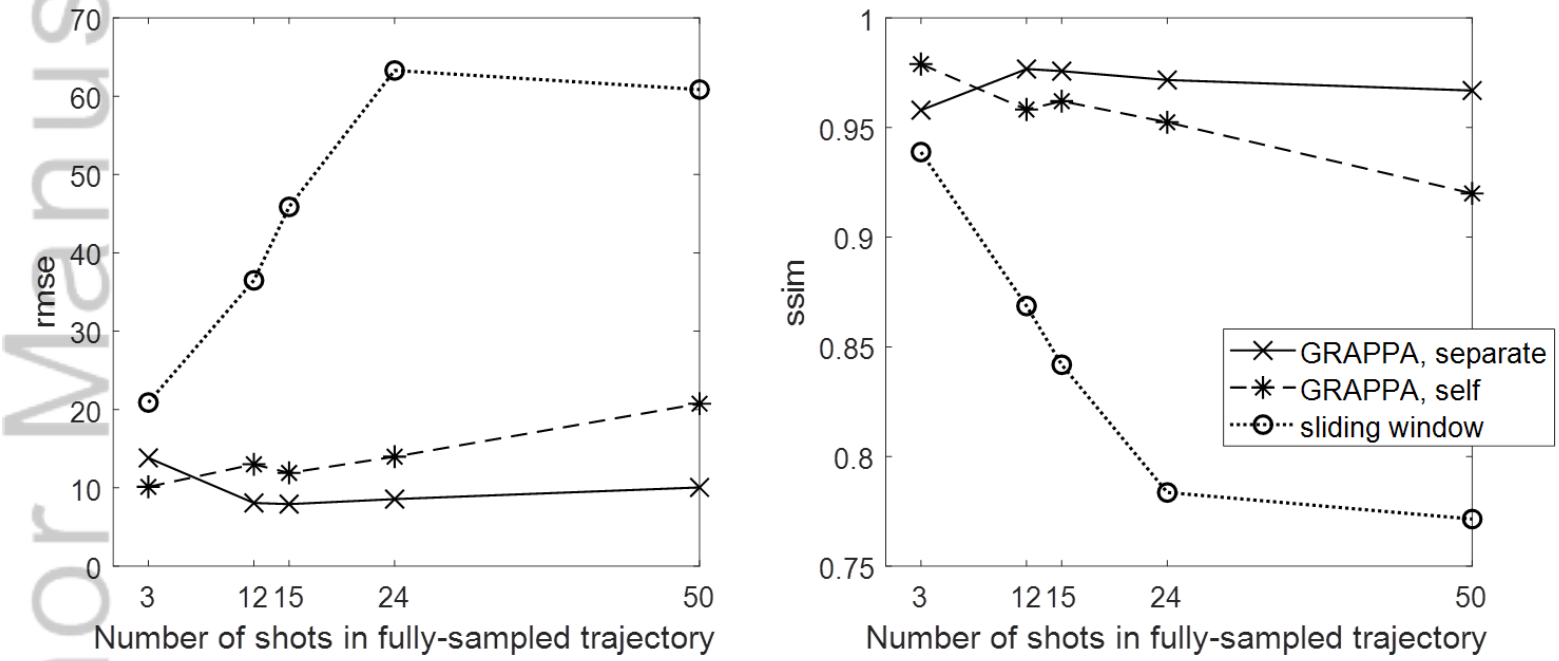

MRM_29462_Figure3.tif

Author Manuscript

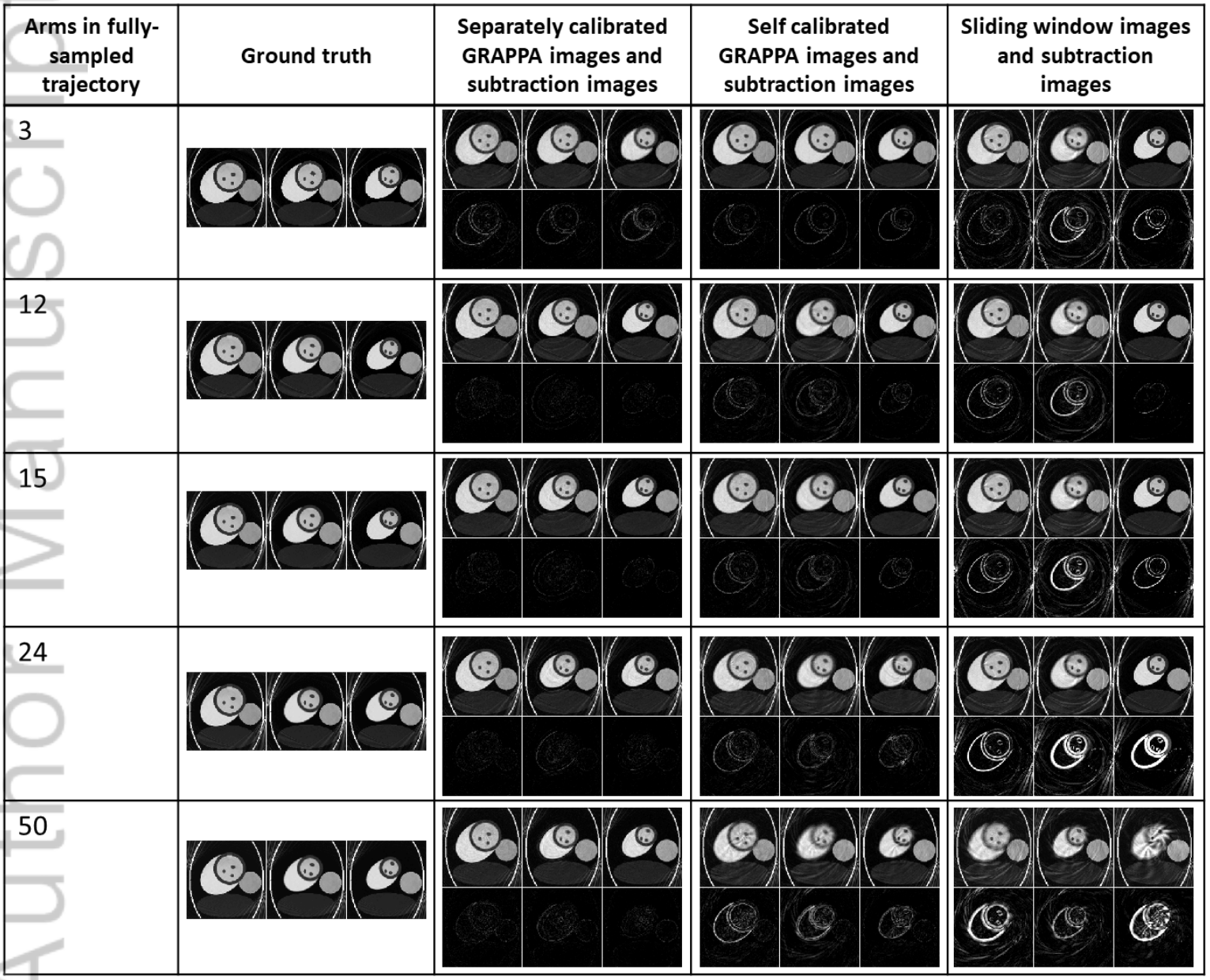

MRM_29462_Figure4.tif

Author Manuscript

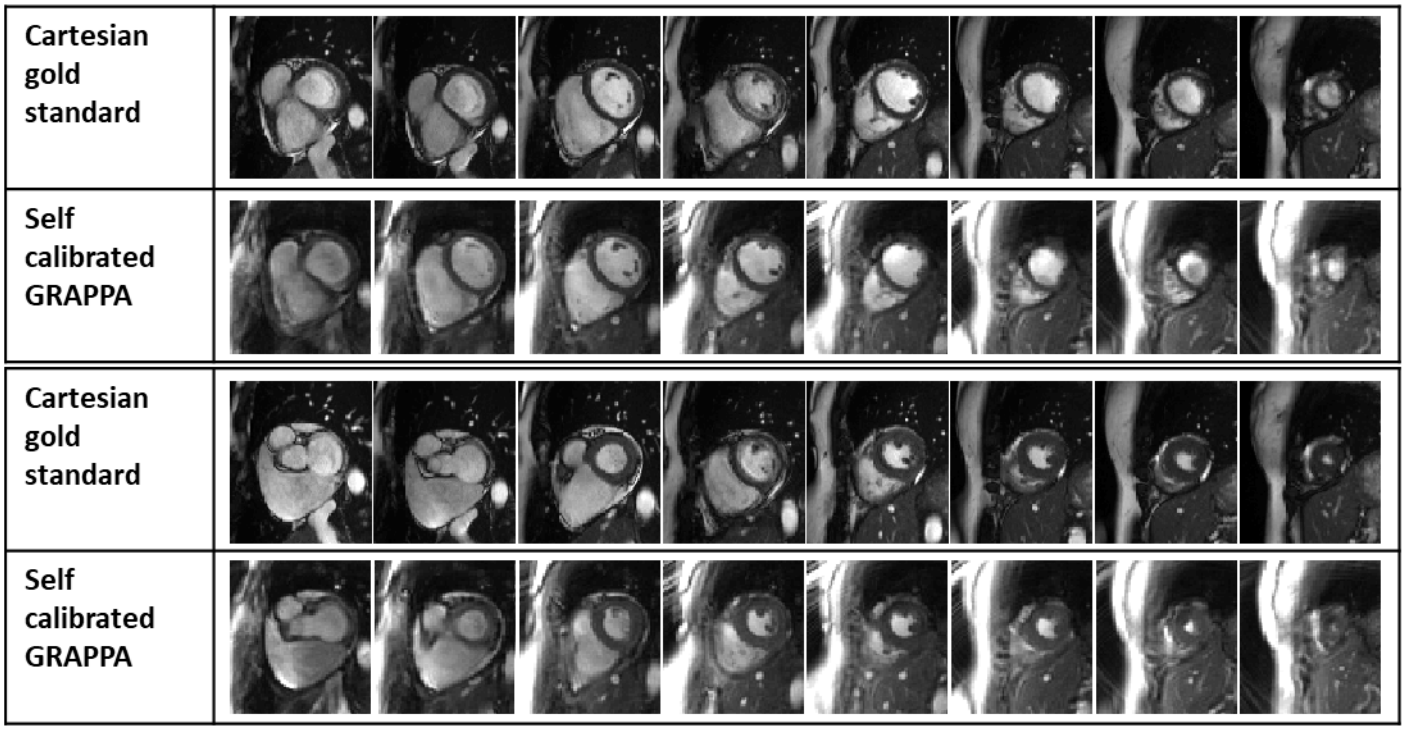

MRM_29462_Figure5.tif

Author Manuscript

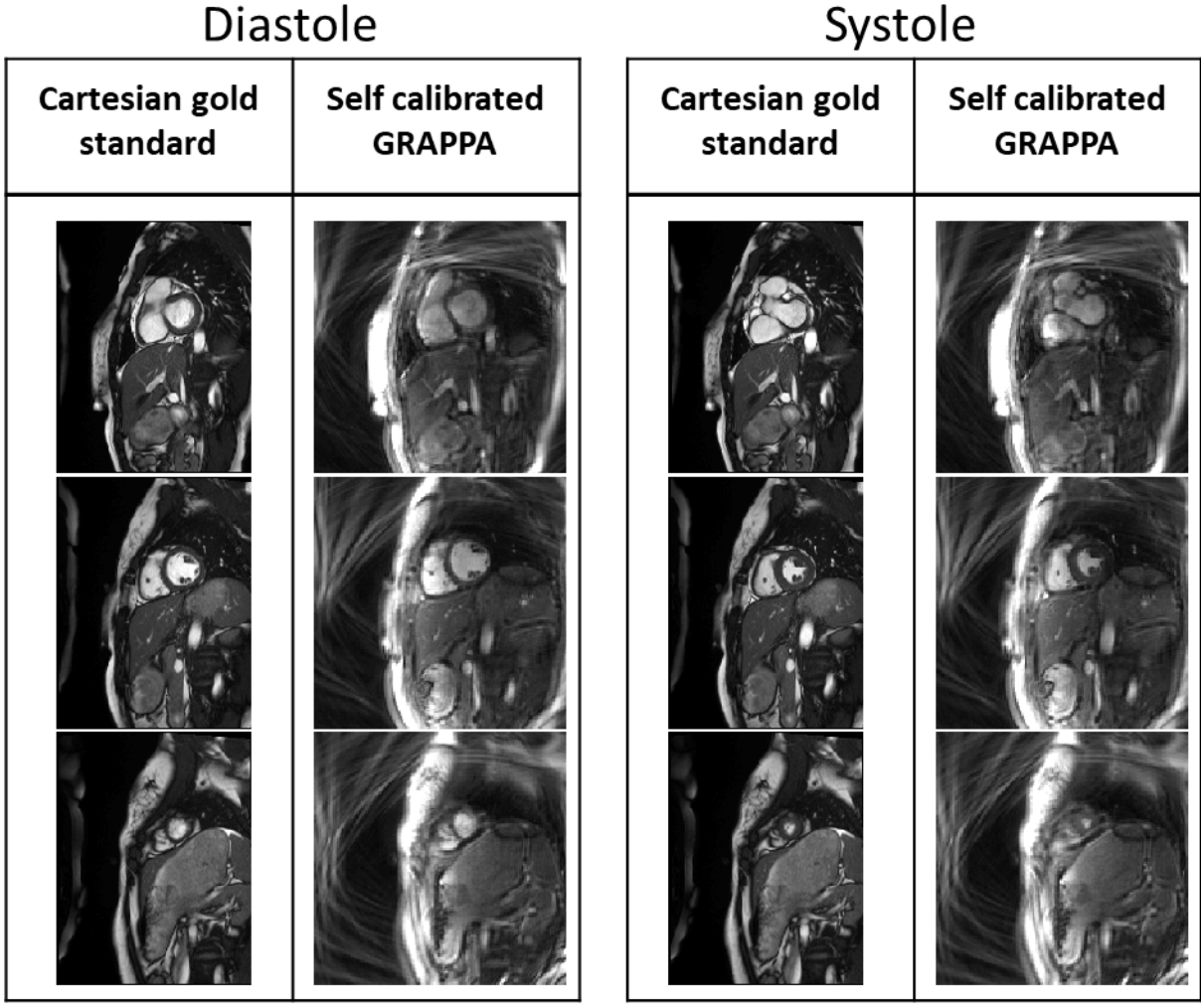

MRM_29462_Figure6.tif

Author Manuscript

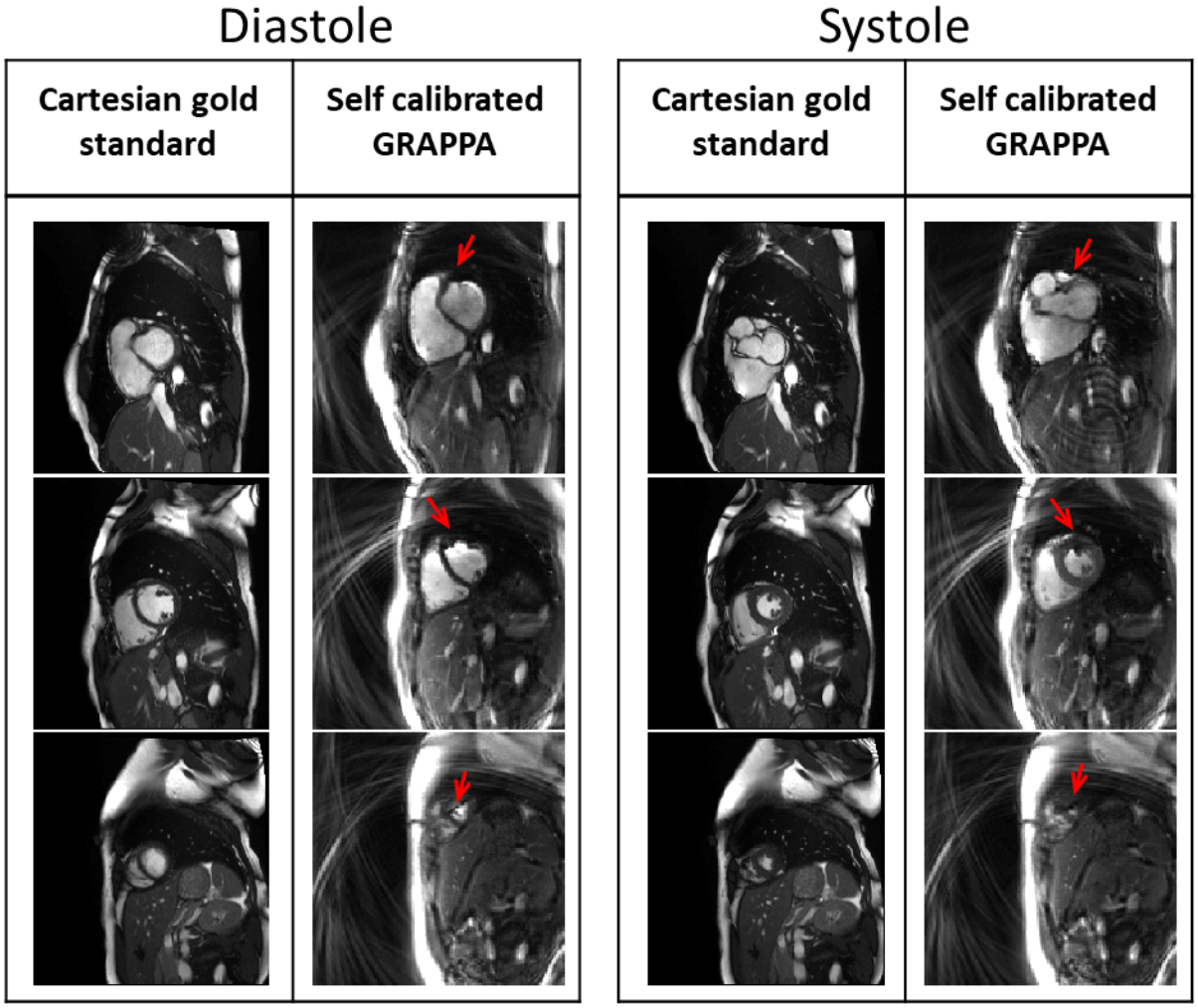

MRM_29462_Figure7.tif

Author Manuscript

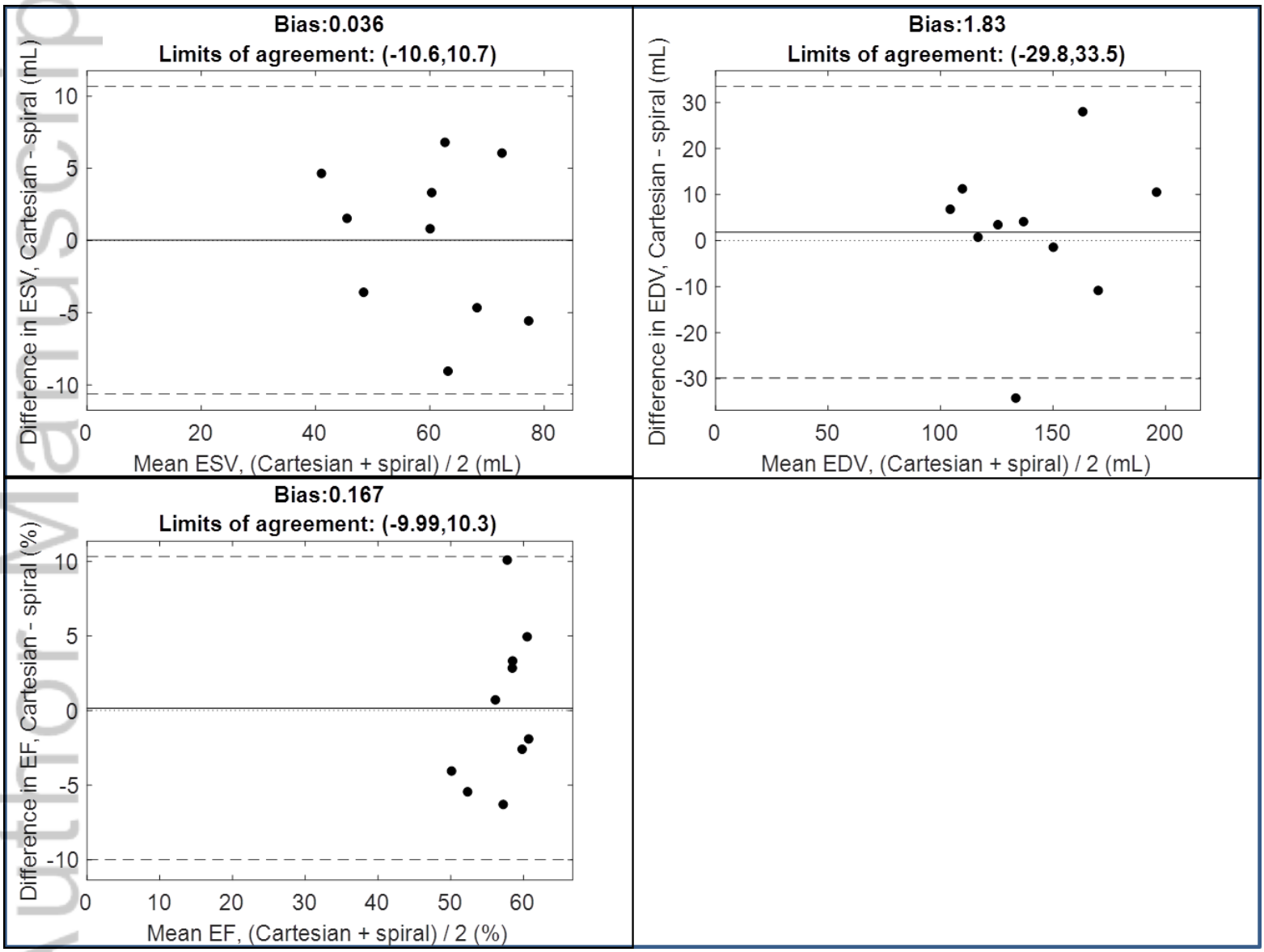

MRM_29462_Figure8.tif

Functional metric	Bland-Altman statistics			Absolute differences		Paired t-test
	Mean bias	Lower limit of agreement (-1.96 SD)	Upper limit of agreement (+1.96 SD)	Mean absolute difference	Maximum absolute difference	p-value
ESV (mL)	0.036	-10.6	10.7	4.60	9.04	0.984
EDV (mL)	1.83	-29.8	33.5	11.1	34.2	0.728
EF (%)	0.167	-9.99	10.3	4.22	10.1	0.921

Table 1: Comparison of functional values calculated using the proposed self-calibrated spiral GRAPPA method and the gold-standard Cartesian cine. Statistics are given over 10 healthy volunteers.

Author Manuscript

Author Manuscript

	Cartesian gold standard	Self-calibrated GRAPPA	pWSR
Level of artifacts	4.1 ± 0.57	2.8 ± 0.63	0.016*
Blood-myocardium contrast	4.6 ± 0.70	3.5 ± 0.53	0.0039*
Sharpness of endocardial border	3.9 ± 0.88	3.1 ± 0.74	0.078
Temporal dynamics of the papillary muscles	4.4 ± 0.84	3.7 ± 0.95	0.17
Temporal dynamics of the left ventricular wall	4.1 ± 1.1	3.8 ± 0.79	0.55

Table 2: Likert scale ratings of different image quality aspects for each of the imaging methods. Mean ± SD over 10 volunteers are given. Each aspect was rated on a 5 point Likert scale (1: non-diagnostic, 2: poor, 3: average, 4: good, 5: excellent). Note that a lower rating for the level of artifacts indicates worse artifacts. The pWSR level is given between the gold-standard Cartesian and the self-calibrated GRAPPA methods. Asterisked values indicate features that were statistically significantly different ($p < 0.05$).